Providing crop information using RADARSAT-1 and satellite optical imagery

H. McNairn[1], J. Ellis[2], J.J. van der Sanden[1], T. Hirose[2] and R.J. Brown[1]

[1] Canada Centre for Remote Sensing
588 Booth St.
Ottawa, Ontario (Canada) K1A 0Y7
heather.mcnairn@ccrs.nrcan.gc.ca
(613) 947-1815 (tel)
(613) 947-1385 (fax)

[2] Noetix Research Inc.
265 Carling Ave., Suite 403
Ottawa, Ontario (Canada) K1S 2E1

Abstract

In 1997, the Canada Centre for Remote Sensing acquired RADARSAT-1, SPOT and IRS-1C imagery over an agricultural site in western Canada. These data were used to address the information content of RADARSAT-1 imagery for mapping crop type and for providing information on crop condition, and to explore the implications of crop growth stage on crop monitoring with radar imagery. The use of radar for crop mapping is particularly attractive because of its all weather capability and the sensitivity of microwaves to canopy structure and moisture. Results from this study indicated that multi-date RADARSAT-1 imagery, with or without satellite optical imagery, can provide accurate information about crop types, although timing of image acquisition was important. Regression analysis established that some indicators of crop vigor – in particular Leaf Area Index and crop height – were correlated with backscatter. The highest correlations were for wheat and potatoes. However, backscatter was insensitive to variations in corn growth and only moderately sensitive to differences in indicators of canola crop condition. Nevertheless, this study clearly demonstrates that multi-temporal RADARSAT-1 imagery can be used to provide useful crop information.

1. Introduction

The vast acreages associated with the global agricultural resource base mean that mapping and monitoring the state of this resource via traditional field surveying is prohibitive. The challenge of monitoring the state of crops and soils is further complicated by their dynamic nature. Crop type varies from field to field and from one season to the next. Crop condition variability is even more significant with the state of the crop varying diurnally and throughout the growing season. Research into the area of precision agriculture has also demonstrated the significant variability in crop condition that is often present within a field.

The spatial and temporal variability associated with crop growth dictates that in many instances, mapping and measuring crop characteristics remotely may be the only viable option. However, the application of remote sensing to crop monitoring requires frequent coverage and often requires data acquisitions during specific critical crop phenological stages. These requirements are true for projects directed towards simple crop type identification, as well as for those involving detailed assessments of the condition of the crop. In promoting remote sensing technology for agricultural mapping and monitoring, the infrequent revisit schedule of earth observation satellites compounded with the obstruction of data collection as a result of cloud cover, has been a significant impediment. However, the all weather capability of Synthetic Aperture Radar (SAR) means that reliability associated with the collection of earth observation data can be greatly enhanced.

The use of visible and infrared sensors to classify crop type and to assess crop acreages has been extensively explored in previous research (see for example, Rosenthal and Blanchard, 1984). Projects like the Large Area Crop Inventory Experiment demonstrated the capability of optical imagery for estimating crop acreages. Further, the dependence of visible and infrared reflectance on plant pigmentation and internal leaf structure led researchers to examine the capabilities of optical sensors for assessing indicators of crop condition. Numerous studies have successfully related various vegetation indices using ratios of red

and infrared reflectances with crop vigour, condition and biomass (Dusek *et al.*, 1985; Gardner *et al.*, 1985; Jasiniski, 1990).

In the microwave region of the electromagnetic spectrum, it is the large scale structure and dielectric properties of the target that influence the amount of energy scattered back towards the sensor. Since crop structure and plant water content vary as a function of crop type, growth stage and crop condition, it is reasonable to assume that SAR sensors would be able to differentiate among crop types and detect changes in crop condition. In fact several previous studies, using primarily ground-based scatterometers or airborne SAR systems, have demonstrated the ability of K-band (Bush and Ulaby, 1978), X-band (Hoogeboom, 1983), C-band (Brown *et al.*, 1992) and L-band (Ulaby et al, 1980) radar to discriminate crop cover classes. Other research has reported the improvement in crop classification when both visible-infrared and active microwave data are used together (Rosenthal and Blanchard, 1984) and has demonstrated the advantages of multi-date visible, infrared and SAR datasets (Brisco and Brown, 1995).

Several researchers have gone beyond the establishment of simple crop classes and have tried to link indicators of crop condition – including canopy moisture, Leaf Area Index (LAI) and biomass weights – to SAR backscatter. These results have generally been encouraging although the correlations have been dependent upon SAR configurations and crop characteristics. Experiments based on truck mounted scatterometers demonstrated the dependence of backscatter on canopy moisture content (Brakke *et al.*, 1981; Ulaby and Bush, 1976), LAI (Brakke *et al.*, 1981; Prevot *et al.*, 1993) and crop dry weight (Brakke *et al.*, 1981). However, optimal incidence angles varied among the results, with recommended angles from steep (20^o) to shallow (70^o).

Although the capability exists, operational implementation of an agricultural monitoring system based on SAR imagery has yet to occur. A system set up to monitor crops would require meteorological and crop growth models that predict crop condition and final yield. Data are required as inputs to these models and operational SAR data could be provided by sensors like RADARSAT-1 and ERS-2. Since optical and microwave sensors respond to very different target characteristics, their role in crop monitoring

can be viewed as complementary. In particular, the all weather capability of SAR sensors can ensure that data gaps that often exist during monitoring with optical sensors are filled. The flexibility associated with RADARSAT-1 beam steering significantly improves the revisit schedule and makes RADARSAT-1 data particularly attractive for agricultural monitoring.

Advances in low cost computing systems, global position satellites, and production of machinery for variable rate seeding, crop inputs, crop protection products, as well as on-the-fly yield monitors have enabled producers and service providers to divide fields into areas of homogenous characteristics and manage each zone separately. Remote sensing is playing an important role in this area because the imagery provides an objective map of the spatial variability and allows monitoring of the crop condition throughout the growing season. Applications of remote sensing that are proving to have a commercial market include i) defining soil management zones representing areas of similar soil characteristics; ii) irrigation scheduling; iii) detecting weeds during pre-emergence, vegetative growth, ripening, and post harvest; and iv) detecting crop stress and damage due to pests, disease, and extreme weather. Soil management zones are used to direct soil sampling and fertility planning. Mapping soil moisture is used to determine irrigation schedules. Crop scouts use the crop condition variability detected by remote sensing to identify the cause and to follow-up with an action plan to reduce the impact of this variability on yield.

The research conducted in previous agricultural studies, in conjunction with potential commercial applications of remote sensing data, suggests that the use of an operational all weather satellite like RADARSAT-1 for agricultural monitoring needs to be explored. This study specifically addresses the following objectives:

1. Examine the capability of RADARSAT-1, as well as visible and infrared imagery, for mapping crop type and identify the optimal timing of image acquisition.
2. Determine the impact of variations in crop growth stage on mapping crop information from remotely sensing imagery.
3. Investigate the sensitivity of RADARSAT-1 and optical sensors to indicators of crop condition.

2. Methodology

2.1 Description of data acquisition

The site used in this study is centred on the town of Carman (98^{o} 00' W longitude, 49^{o} 30' N latitude), located in southern Manitoba (Canada) (figure 1). Both sandy and heavier clayey soils are found across the site and this soil mix is reflected in the diversity of agricultural crops, including canola, wheat, barley, oats, sunflowers, soybeans, corn, potatoes and flax. The Canada Centre for Remote Sensing (CCRS) used this site in 1997 as part of its ongoing program for development of SAR applications in agriculture. As well, this region was also used as the CCRS precision agriculture research site and consequently, quantitative information on site specific crop condition was available.

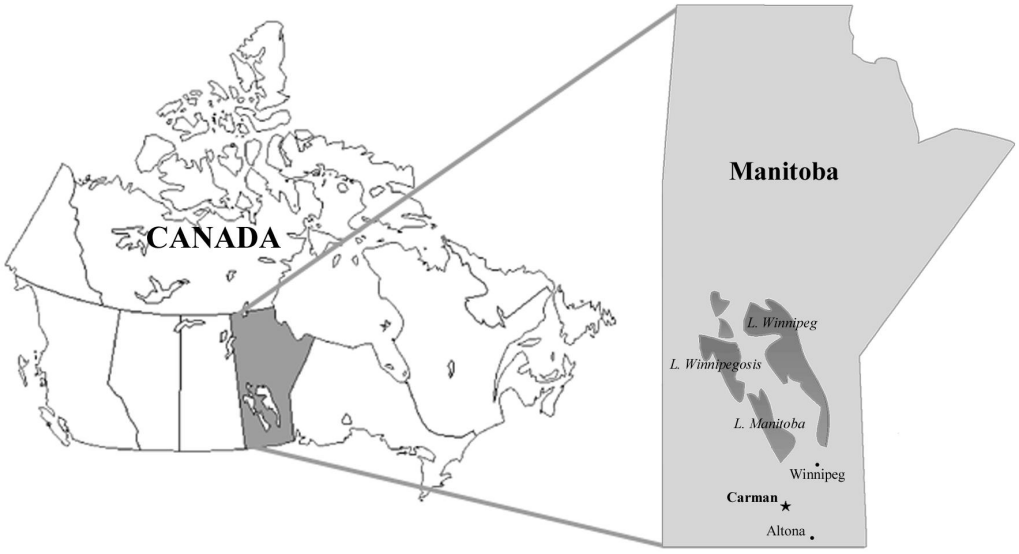

Figure 1. Location of the Carman study site. The town of Carman is situated south and west of Winnipeg, Manitoba (Canada).

A total of 10 Standard and Fine mode descending RADARSAT-1 images were acquired over the Carman area in 1997 during the months of June, July and August (table 1). Available cloud free optical imagery was also acquired and included a SPOT HRV (August 6) and an IRS-1C PAN (July 4) image. Hourly meteorological records were used to assess target conditions at the time of image acquisition.

Table 1. RADARSAT-1 descending and satellite optical imagery acquisition schedule Carman, Manitoba (1997)

Acquisition Date (1997)	Acquisition Mode	Incidence Angle
June 28	Fine 2	39-42^{o}
July 4	IRS-1C PAN	
July 5	Fine 4	43-46^{o}
July 15	Standard 4	34-40^{o}
July 18	Standard 1	20-27^{o}
July 22	Fine 2	39-42^{o}
July 29	Fine 4	43-46^{o}
August 5*$^{+}$	Fine 5	45-48^{o}
August 6	SPOT HRV	
August 8	Standard 4	34-40^{o}
August 15*	Fine 2	39-42^{o}
August 22	Fine 4	43-46^{o}

$^{+}$ Only partial coverage of site
*Meteorological records suggest rain on canopy at the time of acquisition

To characterize field conditions during the 1997 growing season, crop information was collected on July 18-19, 1997 for approximately 300 fields in the Carman area. For each field this included crop type, phenological stage, crop height and percent crop cover. Differential GPS ground co-ordinates were gathered at road intersections at approximately 1.6 km intervals across the study site. Positional accuracies for the GPS model used are well within a RADARSAT-1 Fine Mode pixel (approximately 3-5 metres in the XY direction, 95% of the time). These data were used in the subsequent geocoding of the RADARSAT-1 imagery.

During the same week in which general crop information was documented, field crews also collected information on crop growth across 12 pre-selected fields. On each of the 12 fields, transects were planned across the fields, along which sample sites were located. In general, 8-12 sample sites were located in each field. The location of all within-field sample points was also recorded using a differential GPS. At each sample point along the transect, a number of specific measurements and samples were gathered:

(1) Biomass: At each site, a 0.5 x 0.5 m sample of above ground crop was cut and placed in a plastic bag. Biomass samples were weighed wet in the field, and then oven dried for 48-72 hours and re-weighed. Plant water content (PWC) was calculated using:

$$[(wet\ \ biomass\,(g) - dry\ \ biomass\,(g))/\ wet\ \ biomass\,(g)] \times 100 \qquad (1)$$

(2) Leaf Area Index (LAI): A subsample of plant biomass was used to measure leaf area in the lab with a Li-Cor 3100 area metre. The leaf area of the subsample (LA_{sub}) was used to establish the Leaf Area Index of the 0.5 x 0.5 m sample area through:

$$\left[LA_{sub}\ \ (m) \times \frac{total\ \ wet\ \ weight(g)}{subsample\ \ wet\ \ weight(g)} \right] \div [sample\ area\ of\ \ 0.5\,x\,0.5\,m] \qquad (2)$$

This approach to LAI estimation works well for crops with continuous cover or crops with relatively narrow row spacing (potatoes, wheat, and canola). Table 2 lists the mean, standard deviation and range of values associated with each measured crop variable. LAI measurements for wheat, potatoes and canola agree well with those given in the literature for crops with a similar growth stage (Prévot *et al.*, 1993; Cloutis *et al.*, 1996; Hocheim and Barber, 1997). Corn LAI values were larger than expected. However, since the measurement technique was applied consistently from site to site, relative differences in LAI from one site to the next are valid.

(3) Crop height: At each site, crop height was recorded in centimetres.

Table 2. Summary of variables measured for each crop type

	Number of Sample Points		Height (m)	Wet Biomass (g)	Dry Biomass (g)	Plant Water Content (%)	Leaf Area Index (m^2/m^2)
Wheat	27	Mean	0.60	355.57	80.60	75.04	2.23
		Standard Deviation	0.35	235.27	57.66	12.56	1.10
		Standard Error of Mean	0.07	45.28	11.10	2.42	0.21
		Minimum Value	8	5.0	1.1	67.7	0.4
		Maximum Value	104	767.8	201.2	85	4.3
Potatoes	42	Mean	0.44	561.49	58.25	89.02	2.79
		Standard Deviation	0.14	246.13	23.98	2.35	1.59
		Standard Error of Mean	0.02	37.98	3.70	0.36	0.25
		Minimum Value	10	45.3	8.9	80.4	0.2
		Maximum Value	78	1560.2	127.8	94.4	6.2
Canola	21	Mean	1.13	811.25	106.64	86.19	3.20
		Standard Deviation	0.17	225.85	32.18	2.69	0.80
		Standard Error of Mean	0.04	49.28	7.02	0.59	0.17
		Minimum Value	81	343.3	53.3	80.5	1.9
		Maximum Value	142	1152.2	176.2	89.3	5.3
Corn	21	Mean	1.14	840.32	101.20	87.40	8.89
		Standard Deviation	0.38	408.36	49.81	2.24	4.50
		Standard Error of Mean	0.08	89.11	10.87	0.49	0.98
		Minimum Value	36	120.3	16.5	83.5	0.9
		Maximum Value	152	1603.1	184.8	90.9	16.6

2.2 Data pre-processing and analysis – crop type classification

All RADARSAT-1 imagery used within this project was processed at the Canadian Data Processing Facility (CDPF). This processing included application of the Payload Parameter File corresponding to the acquired imagery. This file contains the antenna elevation gain pattern that is applied during processing to reverse the illumination variation that occurs during imaging. The image quality and

calibration of these data are expected to be consistent with those reported by Srivastava et al. (1999); a relative radiometric accuracy of better than 1.0 dB.

Prior to image analysis, the digital number values were converted to radar brightness (β^o) by reversing the application of a Look Up Table. This Look Up Table had been applied just prior to the data transfer to CD-ROM in the CDPF.

The RADARSAT-1 data were then geocoded using the satellite ephemeris information, ground control points with positions obtained using GPS, and a second order cubic convolution resampling algorithm. The SPOT and IRS images were image-to-image rectified with the SAR images, using the same resampling algorithm.

From the information recorded on the crop survey sheets, masks were drawn over selected homogeneous fields and mean power and reflectance values extracted for each field. The potential of the extracted values for crop type classification was evaluated with the help of a class separability measure known as pairwise transformed divergence (Swain and Davis, 1978). This measure represents the statistical distance between class pairs and is an indirect and *a priori* estimate of the probability of correct classification. The transformed divergence TD for class pair (i, j) is given by:

$$\mathrm{TD}_{ij} = 2\left(1 - e^{\frac{-\mathrm{D}_{ij}}{8}}\right) \tag{3}$$

with

$$\mathrm{D}_{ij} = \frac{1}{2}\mathrm{tr}\left[\left(\boldsymbol{c}_i - \boldsymbol{c}_j\right)\left(\boldsymbol{c}_j^{-1} - \boldsymbol{c}_i^{-1}\right)\right] + \frac{1}{2}\mathrm{tr}\left[\left(\boldsymbol{c}_i^{-1} + \boldsymbol{c}_j^{-1}\right)\left(\boldsymbol{m}_i - \boldsymbol{m}_j\right)\left(\boldsymbol{m}_i - \boldsymbol{m}_j\right)^{\mathrm{T}}\right] \tag{4}$$

where: $\boldsymbol{c}_i$ is the covariance matrix, $\boldsymbol{c}_i^{-1}$ the inverse covariance matrix and $\boldsymbol{m}_i$ the mean vector for class i. Similarly, $\boldsymbol{c}_j$, $\boldsymbol{c}_j^{-1}$ and $\boldsymbol{m}_j$ represent the statistics for class j. The trace of the matrix in question is indicated by tr, whereas T refers to the transposed matrix. Computation of TD_{ij} is based on the assumption that the classes have Gaussian (normal) probability density functions. For the classes studied this assumption will be valid because they are comprised of data points that represent field averaged values. For

the single variate case, that is, when the classification potential is assessed for a single RADARSAT-1 acquisition or a single optical image channel, equation 4 can be rewritten as:

$$D_{ij} = \frac{1}{2}\left(s_i^2 - s_j^2\right)\left(\frac{1}{s_j^2} - \frac{1}{s_i^2}\right) + \frac{1}{2}\left(\frac{1}{s_i^2} + \frac{1}{s_j^2}\right)\left(m_i - m_j\right)^2 \qquad (5)$$

where: m_i, m_j represent the means and s_i^2, s_j^2 the variances of the classes *i* and *j*. However, research such as that reported by Brisco and Brown (1995) has emphasized that successful classification of crops requires multi-temporal/sensor acquisitions. RADARSAT-1 acquisitions that provided high individual TD_{ij} values were therefore assessed further in conjunction with two complementary image channels, that is, one or two RADARSAT-1 acquisitions and/or one or two satellite optical channels.

In the present study, two classes were considered separable if the TD_{ij} value was equal to or greater than 1.9. A TD_{ij} value of 1.9 can be shown to correspond to a lower bound for the likelihood of correct classification of close to 78% (van der Sanden and Hoekman, 1999). Field averaged values associated with 3-channel image combinations that offered good classification potential were then used in Gaussian maximum-likelihood classifications. Successive evaluation of the results by means of confusion matrices and the Kappa coefficient allowed for a direct assessment of the classification capacity of the channels in question (Lillesand and Kiefer, 1994). In contrast to the overall classification accuracy, the Kappa coefficient accounts for errors of omission and commission and the effects of chance agreement. The Kappa coefficient is thus considered a more robust indication of classification accuracy. For each image combination, the same dataset was used for both the design of the classifier and the evaluation of the classification results. The adopted procedure is nevertheless valid (van der Sanden and Hoekman, 1999) since the aim of the study is to assess the relative rather than the absolute classification capacities of the 3-channel image combinations studied. Assessment of absolute probabilities of correct classification requires datasets that are substantially larger than those studied.

2.3 Data pre-processing and analysis – crop condition assessment

In examining the imagery collected over several of the 12 intensively sampled fields, significant within-field variability was detected on several of the image acquisitions. Visual interpretation of the images using field observations suggested that the RADARSAT-1 imagery was showing differences in soil attributes during periods of low vegetative growth and differences in crop growth during more advanced growth stages. The IRS-1C PAN imagery provided good boundary definition of these within-field differences.

In order to quantify this relationship between crop condition and both radar and optical data, site crop variables were regressed against SAR backscatter coefficients and optical reflectance values. Both bivariate and multivariate linear regression models established the significance and direction of the relationship between crop variables (height, biomass, plant water content and Leaf Area Index) and the remotely sensed data. Fields with the same crop type were pooled together and the crop types examined in this analysis included wheat, potatoes, canola and corn. Since grain crops were senescing in early August, imagery acquired during August was not used in this analysis. All crops were generally in their vegetative or seed development phases during the late-June to late-July time frame. Only the Fine Mode acquisitions were examined since these data provided the necessary spatial resolution and incidence angles for evaluating the sensitivity to within field crop variability.

Prior to extracting site specific backscatter coefficients, each of the 1-look Fine Mode images was filtered using a 3x3 Frost filter in order to reduce speckle effects. The equivalent number of looks in the resulting images was approximately 2.5. Once the GPS locations of the sample sites were overlayed on the geocoded imagery, site specific backscatter and reflectance values could be extracted. In response to locational errors associated with image georeferencing and to residual speckle effects, mean backscatter and reflectance values were based on a 10x10 pixel window centred on each within field site. This 100-pixel sample, coupled with the filtering, sufficiently reduced speckle effects. The effect of speckle on the

mean backscatter values computed for these 100-pixel samples is well within the bounds of within scene radiometric accuracy (Hoekman, 1990).

As described previously, 0.5 x 0.5 m samples of crop biomass were collected during ground data acquisition. Relative to the size of each pixel, these crop samples are small. However, sample sites were chosen within the field to be representative of the surrounding crop area. Although a regression approach that uses measured crop data is required to establish the sensitivity of SAR and optical imagery to crop condition, several factors including geometric inaccuracies and the relatively small biomass sample sizes can create uncertainties within the statistical models. These uncertainties will account for some of the unexplained error in the regression analysis.

3. Results and discussion

3.1 Crop type classification: transformed divergence statistics based on a single RADARSAT-1 image

Divergence statistics were calculated for all of the Carman image acquisitions. Results for the best two RADARSAT-1 dates are presented in table 3. All SAR acquisitions except July 18 (Standard Mode 1) were at angles greater than 35^{o}. At these larger incidence angles, interaction between the microwaves and the crop canopy is maximized. For the Standard Mode 1 acquisition, poor separability was observed among all crop types. The poor crop class separability at steep SAR angles is likely a function of the increased penetration through the crop canopy and the greater contribution to total backscatter from the soil surface. This penetration results in less dependence of the backscatter on crop variables.

Although the Standard Mode 1 acquisition indicated the difficulty in crop classification due to the confounding contributions associated with the canopy and soil, the timing of acquisition during the growing season is also critical. Divergence statistics derived for the RADARSAT-1 imagery collected early in the growing season (late June to early July) indicated poorer separation among most crops. With the relatively low vegetative cover, significant soil contributions likely still exist even though incidence angles were large (greater than 35^{o}).

The only exception was canola (June 28) which was separable from barley and corn at this early growth stage. For this late June acquisition, the canola crop covered most of the soil surface, providing greater interaction of the microwaves with the crop and less soil contributions. However for all other crop comparisons, it was not until late July that some separability was observed, using a single RADARSAT-1 image. In this agricultural region during late July to early August, crops have completed their vegetative growth period and are now in their reproductive and seed development stage. During this stage, canopy moisture content and canopy structures change dramatically. Brisco and Brown (1995) also reported the enhanced separability of crops during the reproductive and seed development stage for a similar site in the Canadian Prairies.

With a single late July to early August RADARSAT-1 image, broadleaf crops were generally separable from small structured crops. However, backscatter within the broadleaf crop class was similar. For example sunflowers, with their large distinctive leaves, stalks and heads, had a backscatter significantly different from the small structured grain crops. However, it was more difficult to separate sunflowers from other broadleaf crops that also have large leaf and stalk structures. Thus separation of crops beyond 2 classes – broadleaf and small grains – would be difficult using only a single RADARSAT-1 image.

In examining each individual RADARSAT-1 image, the late July/early August time period was best for crop type discrimination. This compares well with Brisco and Brown (1995) who found that the highest multi-date crop classification accuracy for C-HH included a July 21st and an August 10th acquisition. Using three images the authors were able to classify crops to a 72% overall accuracy.

Table 3. Transformed divergence results for best two RADARSAT-1 dates

July 22 (RADARSAT-1 Fine 2) (39-42°)

	Barley	Beans	Canola	Corn	Flax	Oats	Sunflower
Beans	1.82						
Canola	1.69	0.05					
Corn	1.77	0.01	0.02				
Flax	0.04	1.67	1.50	1.61			
Oats	0.01	1.92	1.83	1.89	0.08		
Sunflower	2.00	1.05	1.61	1.35	2.00	2.00	
Wheat	0.34	0.77	0.64	0.73	0.18	0.50	1.90
						Average Divergence:	1.11

August 8 (RADARSAT-1 Standard 4) (34-40°)

	Barley	Beans	Canola	Corn	Flax	Oats	Sunflower
Beans	0.87						
Canola	1.35	0.62					
Corn	0.63	0.00	0.46				
Flax	0.43	2.00	2.00	2.00			
Oats	0.08	1.51	1.90	1.34	0.08		
Sunflower	1.80	1.55	0.37	1.25	2.00	1.99	
Wheat	0.05	0.46	0.98	0.30	1.66	0.35	1.56
						Average Divergence:	1.06

3.2 Crop type classification: transformed divergence statistics based on three channel combinations

Although analysis of single date imagery suggested that some crop classes could be separated, these results clearly indicate that multi-date imagery would be required to classify crop type at an acceptable level of accuracy. To address this requirement divergence statistics were regenerated based on three channel combinations of SAR, SPOT and IRS imagery. Both divergence (table 4) and field based classification (table 5) results are provided.

Divergence statistics and classification accuracies (tables 4 and 5) are presented for only those image combinations with Kappa coefficients exceeding 0.80. Separation among small grain crops (oats,

barley, and wheat) based on SAR backscatter is difficult due to the crops' very similar structures. Divergence statistics were first generated with individual grain classes maintained and were then calculated after pooling the fields of oats, barley and wheat into a single small grain class.

The three-channel comparisons of crop separability supported the divergence measures calculated using a single SAR acquisition or single optical channel. Using a mid-season SAR acquisition (July 22) coupled with late season SAR data or an IRS PAN or SPOT HRV acquisition, greater than 80% overall classification accuracies were achieved. The best combinations used either two or three dates of RADARSAT-1 and the IRS-1C acquisition. With these choices, both the transformed divergence statistics and the classification results demonstrated excellent crop separation, particularly if grain crops are pooled into a single class. The transformed divergence numbers confirm significant confusion among wheat, barley and oat fields, when both optical reflectance and microwave backscatter data are used. Even once pooled, the grain class had the highest classification errors, most likely related to the significant variability observed within this class. Differences in grain crop varieties and significant differences in crop growth stages contributed to high within class variability. The multi-temporal image provided in figure 2 illustrates that RADARSAT-1 is detecting a large number of crop classes. These classes are primarily related to crop type differences. However, growth stage and crop condition are also contributing to backscatter differences.

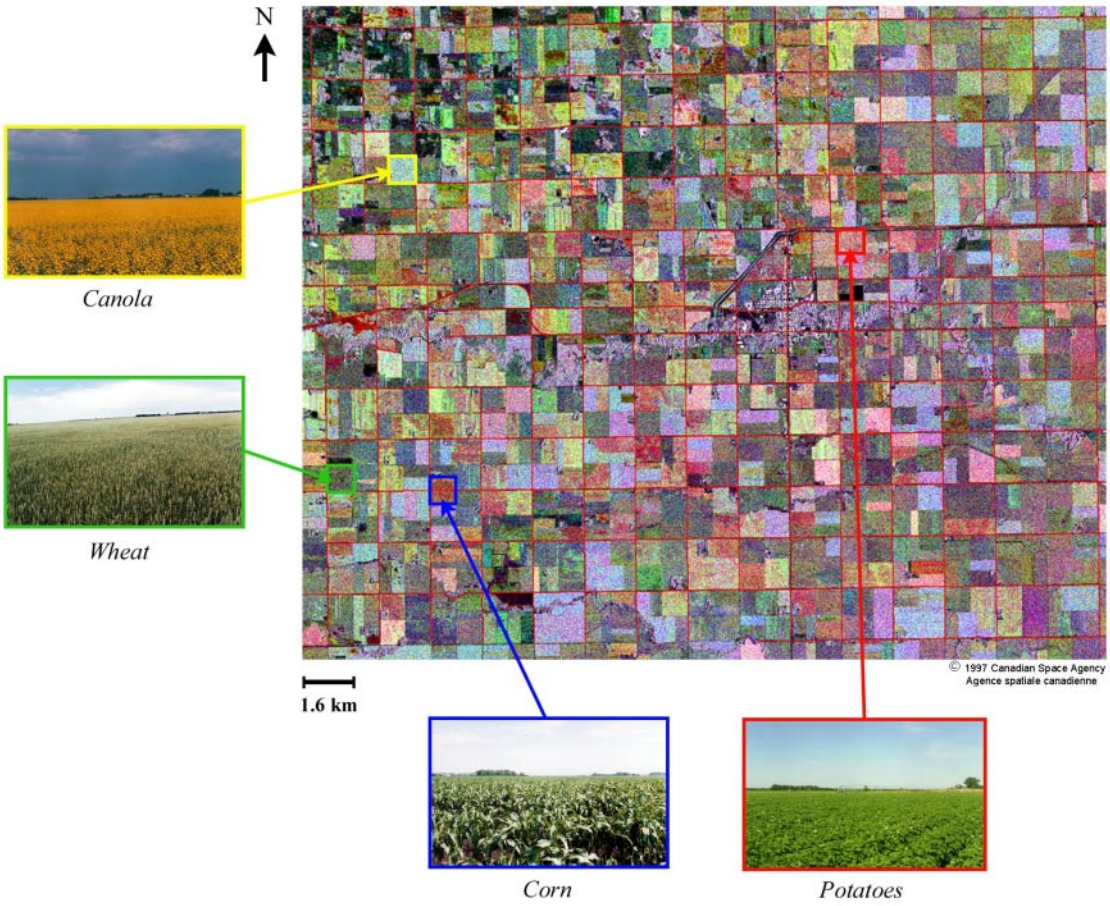

Figure 2. RADARSAT-1 colour composite of the Carman study area. This three-date multi-temporal image is a composite of July 22 (F2) displayed in red, July 5 (F4) displayed in green and June 28, 1997 (F2) displayed in blue. A number of different crop classes are obvious. The differences in backscatter from one field to the next are a result of not only crop type, but also growth stage and crop condition.

Of note is the relatively poor classification performance of the three-channel SPOT image. The Kappa coefficient for this multi-channel image was low (0.66) and most crops were poorly classified with the exception of corn and canola. The flowering and podding of the canola crop at the time of the SPOT acquisition results in significant changes in crop reflectance and likely explains the better separability associated with this crop. Timing of optical image acquisition in reference to crop growth stages is important and the early August SPOT acquisition is not optimal for crop discrimination (Bober *et al.*, 1996). However, persistent cloud cover that occurred over the site during the month of July reinforces the advantages of SAR in agricultural monitoring.

Table 4. Transformed divergence results for three channel combinations of satellite optical and RADARSAT-1 imagery

IRS PAN July 4
RADARSAT-1 July 22
RADARSAT-1 August 8

	Wheat	Barley	Beans	Canola	Corn	Flax	Sunflower
Oats	0.90	0.33	2.00	2.00	2.00	1.70	2.00
Wheat		0.41	1.87	1.98	1.90	1.95	2.00
Barley			1.98	2.00	1.99	1.99	2.00
Beans				2.00	1.51	2.00	1.96
Canola					1.95	2.00	2.00
Corn						2.00	1.98
Flax							2.00
Grains			1.88	1.98	1.93	1.94	2.00

IRS PAN July 4
RADARSAT-1 July 22
RADARSAT-1 August 22

	Wheat	Barley	Beans	Canola	Corn	Flax	Sunflower
Oats	0.80	0.94	2.00	2.00	2.00	1.13	2.00
Wheat		0.99	1.89	1.96	1.98	1.46	2.00
Barley			2.00	1.99	2.00	2.00	2.00
Beans				2.00	1.78	2.00	2.00
Canola					1.99	2.00	2.00
Corn						2.00	2.00
Flax							2.00
Grains			1.93	1.98	1.99	1.10	2.00

RADARSAT-1 July 22
RADARSAT-1 August 8
RADARSAT-1 August 22

	Wheat	Barley	Beans	Canola	Corn	Flax	Sunflower
Oats	0.92	1.21	2.00	2.00	2.00	1.78	2.00
Wheat		1.05	1.82	1.98	2.00	1.98	2.00
Barley			2.00	1.99	2.00	2.00	2.00
Beans				1.94	1.51	2.00	2.00
Canola					1.99	2.00	2.00
Corn						2.00	2.00
Flax							2.00
Grains			1.84	1.99	2.00	1.96	2.00

Table 4 con'd. Transformed divergence results for three channel combinations of satellite optical and RADARSAT-1 imagery

SPOT Channel 3 August 6
RADARSAT-1 July 22
RADARSAT-1 August 8

	Wheat	Barley	Beans	Canola	Corn	Flax	Sunflower
Oats	0.90	0.91	2.00	2.00	2.00	1.87	2.00
Wheat		0.69	1.62	1.99	1.96	1.99	2.00
Barley			1.96	2.00	2.00	2.00	2.00
Beans				1.59	1.18	2.00	1.66
Canola					1.98	2.00	1.99
Corn						2.00	2.00
Flax							2.00
Grains			1.67	1.98	1.97	1.98	2.00

Three Channel SPOT (August 6)

	Wheat	Barley	Beans	Canola	Corn	Flax	Sunflower
Oats	0.32	0.84	1.42	1.90	2.00	1.09	1.83
Wheat		1.00	1.53	1.92	2.00	1.23	1.84
Barley			2.00	2.00	2.00	1.56	2.00
Beans				1.79	1.29	0.73	1.33
Canola					1.92	1.95	0.90
Corn						1.92	1.54
Flax							1.71
Grains			1.80	1.97	2.00	1.22	1.97

Table 5. Field based classification accuracies

3 Channel Combinations	**Corn**	**Flax**	**Grain**	**Sunflower**	**Beans**	**Canola**	**Overall Accuracy**	**Kappa Coefficient *(Grains Separated)***	**Kappa Coefficient *(Grains Pooled)***
IRS PAN (July 4) *July 22 & August 8 Radarsat-1*	83%	100%	81%	100%	100%	97%	88%	0.64	0.84
IRS PAN (July 4) *July 22 & August 22 Radarsat-1*	100%	100%	75%	100%	100%	97%	87%	0.62	0.83
July 22, August 8 & August 22 Radarsat-1	94%	100%	77%	100%	100%	94%	87%	0.70	0.82
SPOT Channel 3 (August 6) *July 22 & August 8 Radarsat-1*	94%	100%	80%	100%	50%	97%	87%	0.70	0.82
3 channel SPOT (August 6)	83%	14%	75%	70%	33%	91%	75%	0.60	0.66

3.3 The influence of crop growth stage

Figure 3 illustrates the changes in backscatter as a function of changes in the growth stage of canola. In this example, differences in backscatter are evident within a single canola field. Parts of this field were planted on three different dates. As the canola crop forms pods, the crop structure changes dramatically, and backscatter increases. On July 22nd, for the top section of the field where the canola had already podded, backscatter was higher relative to the centre of the field where the crop was still flowering. However, backscatter increased in this centre section later in August once this part of the field reached the podding and ripening stage.

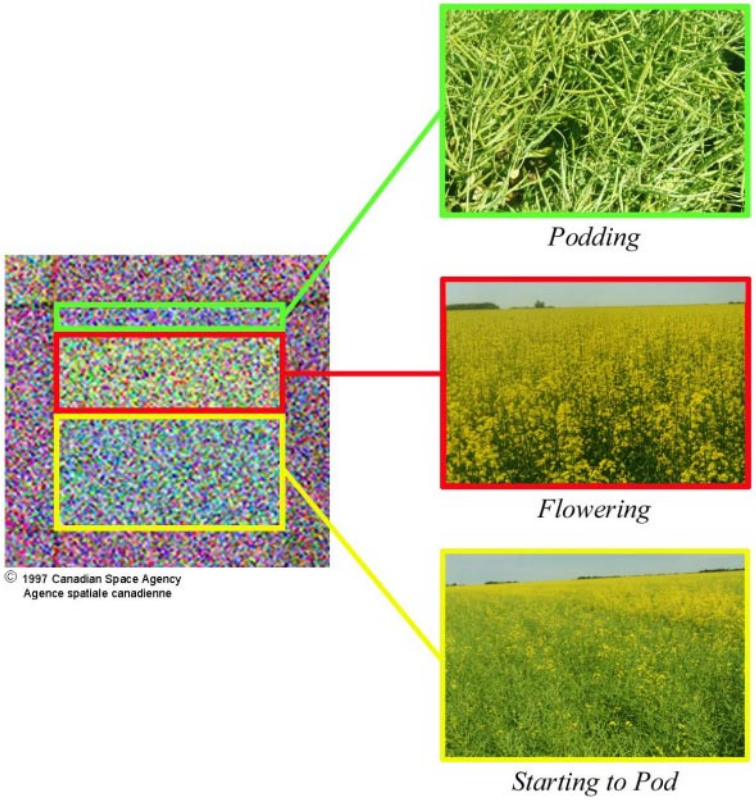

Figure 3. The effect of growth stage of a canola crop on RADARSAT-1 backscatter. In this figure, three dates of Fine Mode RADARSAT-1 imagery have been combined (August 15th displayed in red, June 28th displayed in green and July 22nd displayed in blue). Parts of this canola field were planted at three different times. As a result, the field is segmented into three areas, each at a different crop growth stage. This image illustrates that as the canola changes from flowering to a podding stage, the change in crop structure results in an increase in backscatter.

To further explore the effect of developmental stage on SAR return, fields were grouped by growth stage and mean backscatter was calculated for all grain and canola fields. The effect of changes in crop structure and moisture on backscatter is evident in figure 4. Some changes in backscatter from one growth stage to the next are within the sensor calibration uncertainty. However, the Carman data demonstrate that backscatter decreases once the grain crops head. As well, the increase in backscatter associated with a change in canola from flowering to podding as seen in figure 2, is observed for other fields in the site. Although these changes represent only 1-2 dB, the influence of developmental stage on SAR backscatter must be considered during crop monitoring.

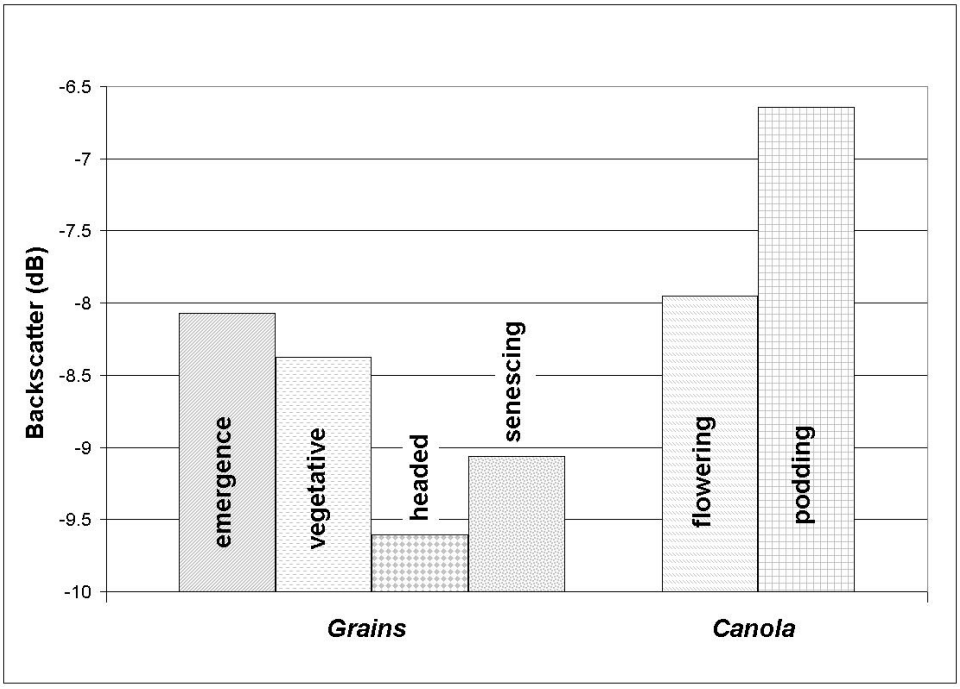

Figure 4. Variation in radar backscatter as a function of the growth stage of canola and grain crops. These mean backscatter values were derived from the July 22nd (1997) RADARSAT-1 Fine Mode acquisition.

As presented in table 3, for single-date imagery, divergence numbers were particularly low for spring grains. Brisco and Brown (1995) also reported poor separability of grain crops and suggested that this was due to the very similar structure among the various grain classes. For the data presented here, class confusion was likely also related to the large variability in backscatter responses associated with the spring wheat class. As evident in figure 4, at the time of field data collection wheat crops across the site were in

various stages of growth including vegetative growth, heading, and senescing. These variations were primarily a result of slight differences in planting dates and to a lesser extent, differences in soil characteristics. This variation within the wheat class suggests that information on the developmental stage would likely be required for the classification of grains. Crop development could be tied to planting date, derived from an early season image acquisition and knowledge of the local crop calendar.

3.4 Crop condition assessment

As evidence of the sensitivity of RADARSAT-1 data to indicators of crop vigor – height, biomass, plant water content and LAI – bivariate correlation coefficients are provided in table 6. These coefficients are based upon site specific measurements (generally 10-12 sites per field) gathered for a number of different crops including wheat (3 fields), potatoes (3 fields), canola (2 fields) and corn (2 fields). In table 6, bivariate correlation results based on the linear regression of crop variables against backscatter are provided separately for the wheat, potatoes and canola crops. Coefficients derived for the corn crop are not provided as none of the correlations were significant at a probability level less than 0.05. Saturation of the SAR signal, or at least reduced sensitivity to increases in canopy biomass, may explain the poor results associated with the corn canopy. For example, although the variance associated with corn canopy height (cm) was high (standard deviation of 38.06) the backscatter (dB) associated with these measurement points on the July 22nd acquisition did not vary a great deal (standard deviation of 0.77). Ferrazzoli *et al.* (1992) reported that at L-band, HH-polarized backscatter from corn and sunflower crops increased with LAI, but saturated once LAI reached the value of 2-3. Further plant growth had little or no effect on backscatter. The relatively large LAI values associated with the corn canopies (table 2) suggest that a similar saturation effect may be occurring. However, this saturation does not occur for all crops. Prévot *et al.* (1993) indicated that no saturation of C-HH backscatter was observed with increasing LAI for wheat canopies, even though LAI was high (LAI > 4).

Regressions were run for only the June 28th and July acquisitions since senescence of grain crops was occurring in August. Although coefficients from as early as June are given, correlation results are

likely more valid during the period closest to the ground data acquisition (third week of July). With crop growth, values for each crop variable (height, biomass, water content and LAI) will be different for each SAR acquisition. Measurements were made only once in the growing season and therefore, extrapolation of results to other SAR acquisitions relies on the assumption that site to site differences in these crop variables remains relatively constant.

The bivariate results provided in table 6 suggest that on a number of dates, crop variables are significantly correlated with C-HH backscatter, particularly for the wheat and potato crops. In general, these crop variables accounted for approximately 25-50% of variability in backscatter. The most significant correlations are observed for crop height and LAI. Cloutis *et al.* (1996) also reported the significance of these two variables for C-HH SAR data acquired on an airborne platform. As well, the strength of the bivariate correlations for the RADARSAT-1 data examined in the present study is similar to those given by Cloutis.

As with these RADARSAT-1 results, Cloutis *et al.* (1996) reported that the strength of the correlations was crop type dependent. The changes in the geometric and dielectric properties of the crop during its vegetative, reproductive and seed development stages are extremely complex, and these changes are crop type dependent. Although these two SAR studies attempt to characterize crops with very simple measures, it remains difficult to capture these physical changes in a single crop variable. As suggested from this study, for some crops like canola, these changes may be more difficult to parameterize.

Table 6. Correlation coefficients established between RADARSAT-1 backscatter and indicators of crop vigor

	Date of Radarsat Acquisition	Simple Correlation Coefficients (R Values)					Multiple Correlation Coefficients (R Values)
		Crop Height	Wet Biomass	Dry Biomass	Plant Water Content	Leaf Area Index	Height, Wet Biomass and LAI
Wheat	June 28	0.67*	0.40	0.39	-0.51*	0.48*	0.87*
	July 5	0.44	0.02	0.03	-0.30	0.04	0.17
	July 22	-0.69*	-0.65*	-0.65*	0.31	-0.61*	0.76*
	July 29	-0.91*	-0.83*	-0.81*	0.45*	-0.80*	0.92*
Potatoes	June 28	0.71*	0.41*	0.64*	-0.44*	0.73*	0.84*
	July 5	0.63*	0.33*	0.53*	-0.43*	0.67*	0.85*
	July 22	0.67*	0.41*	0.53*	-0.31*	0.66*	0.84*
	July 29	0.70*	0.34*	0.50*	-0.31*	0.66*	0.82*
Canola	June 28	0.76*	-0.27	-0.56*	0.36	0.03	0.79*
	July 5	0.59*	-0.39	-0.34	-0.08	-0.11	0.66*
	July 22	-0.07	-0.05	-0.19	0.29	-0.07	0.10
	July 29	0.18	-0.25	0.05	-0.42	-0.29	0.60

* Correlation coefficients are significant at $p < 0.05$

In general, RADARSAT-1 backscatter was positively correlated with measured crop variables, but with two notable exceptions. Although researchers like Brakke *et al.* (1981) have reported positive correlations in similar studies, the Carman wheat samples with greater biomass, LAI and height had lower C-HH backscatter for the late July RADARSAT-1 acquisitions. This reversal in the backscatter relationship is likely related to the change in wheat structure during this period. Wheat plants that are further along in their development are now heading. This change in crop geometry can lead to a decrease in backscatter (Bouman, 1991; Bouman and van Kasteren, 1990) and can effectively override expected increases in backscatter with increases in crop biomass. The effect was also evident in figure 4.

In an early study, Ulaby and Bush (1976) were surprised to find that as plant water content in wheat decreased, backscatter actually increased. The researchers hypothesized that the decrease in attenuation within the wheat canopy allowed the radar to "see" more of the wet underlying soil, resulting in

increased backscatter. Cloutis *et al.* (1996) also attributed inverse relationships to the influence of underlying soil characteristics. The negative correlations between backscatter and plant water content for earlier stages of wheat and potato may also be attributable to similar soil influences. Meteorological data indicated rainfall and cool temperatures in the days prior to the June 28 and July 5th acquisitions. The relatively weak correlations between plant water content and C-HH backscatter is most likely attributable to diurnal patterns and fluctuations in plant water content from day to day. Brisco et al. (1990) found that wheat plant water content can vary between 2-5% over a 24 hour period. As well, from early in the growing season (late June) to mid-July wheat total plant moisture content can increase by a factor of four (Hochheim and Barber, 1997). These results indicate that knowledge of the crop calendar is critical in assessing crop condition from SAR.

The coefficients provided in table 6 suggest that multiple crop variables are required to fully explain variations in backscatter. Both dry biomass and plant water content are derived from wet biomass and consequently, these two variables were not included in the multivariate approach. The multiple correlation coefficients are also listed in table 6.

In comparing the bivariate and multivariate correlation coefficients, it is obvious that in almost all cases, the amount of explained variance increases as more than one crop characteristic is taken into account. As reflected in the simple regressions, the wheat and potato crops produced the best results. For these crops, these three crop variables now account for as much as 85% of the variation in C-HH backscatter. The difficulty in detecting differences in corn condition from backscatter persisted.

The sensitivity of a multi-spectral SPOT image to crop condition variation is established in table 7. Results from a multivariate model that incorporates an early and mid season RADARSAT-1 image are also listed. By including a second RADARSAT-1 image, the unexplained variance for the wheat and potato crops is reduced. However, no improvement is observed in the performance of the model for either the canola or corn canopies. The July 29th acquisition was particularly important in defining differences in the wheat crop. The larger contribution of this date to the model may be related to the rapidly changing wheat

structure at the time of this later acquisition. Both RADARSAT-1 dates contributed equally to the multivariate model for the other crop types.

In comparing regression results using a multi-spectral SPOT image with those derived from the multi-temporal RADARSAT-1 dataset, the strength of the correlations with crop indictors are similar. This observation suggests that the acquisition of an early and mid season RADARSAT-1 pair can provide similar information about crop condition, when compared with a late season multi-spectral optical image.

Table 7. Regression results using multi-temporal RADARSAT-1 data in comparison with SPOT multi-spectral data

	Crop Variable	3 Channel SPOT (August 6 Acquisition) Multiple Correlation Coefficients (R Values)	Radarsat-1 (June 28 and July 29 Acquisitions) Multiple Correlation Coefficients (R Values)
Wheat	Height	0.96*	0.92*
	Wet Biomass	0.89*	0.89*
	LAI	0.88*	0.86*
Potatoes	Height	0.76*	0.78*
	Wet Biomass	0.51*	0.49*
	LAI	0.80*	0.75*
Canola	Height	0.69*	0.59*
	Wet Biomass	0.43	0.37
	LAI	0.43	0.30
Corn	Height	0.70*	0.24
	Wet Biomass	0.51	0.41
	LAI	0.51	0.45

* Coefficients are significant at $p < 0.05$

4. Conclusions

Results from the study presented here indicate that multi-date RADARSAT-1 imagery, with or without satellite optical imagery, can provide accurate information about crop types. Timing of image acquisition is important and the greatest success at separating crop types was achieved with imagery

gathered during the period of seed development. As expected, larger incidence angles, like those associated with RADARSAT-1's Fine Beam Modes, are required to establish crop type. The greatest confusion is observed among the various grain crops (wheat, barley, and oats). The similar structure associated with wheat, barley and oats contributes to confusion among these crop types. Field observations suggested that within this grain class, growth stage varied primarily as a result of differences in planting date. This increased class variability results in some confusion between the grain and broadleaf crops. Nevertheless, good classification accuracies were obtained. The poorer classification results associated with the SPOT image are likely related to the relatively late acquisition (August 6). However the difficulty in acquiring cloud free optical imagery over this site earlier in the season reinforces the advantages of SAR in crop monitoring.

Regression analysis established that some indicators of crop vigor – in particular Leaf Area Index and crop height – were moderately correlated with radar backscatter. If crop height, biomass and Leaf Area Index are used together to define crop condition and are included in a regression model, as much as 85% of the variance in C-HH backscatter is explained. Since bivariate and multivariate results were highly dependent on crop type, classification of crop type is required prior to interpretation of crop condition. Results were encouraging for wheat and potato crops. However, backscatter was insensitive to variations in corn growth and only moderately sensitive to differences in these indicators of canola crop condition. A pair of early and mid season RADARSAT-1 images provided similar correlation results with crop indicators when compared with a multivariate model using three channels of an acquired SPOT image.

Imagery gathered by Synthetic Aperture Radars can provide crop type and crop condition information. However, for SARs like RADARSAT-1 (C-HH) and ERS-2 (C-VV) that acquire data in only a single frequency and polarization, multi-temporal datasets are required. Future space-borne SARs such as RADARSAT-2 and Envisat ASAR will provide imagery in multiple polarizations. These sensors promise to significantly improve the amount of crop information provided in a single acquisition and will be exciting new tools for crop monitoring.

Acknowledgements

The RADARSAT-1 imagery used in this analysis was supplied through the ADRO program (project # 32). Jean-Claude Deguise (CCRS), Josée Lévesque (MIR Télédétection) and Duncan Wood (Radarsat International) helped in gathering field data in Carman. Thanks as well to Dr. Rene van Acker at the University of Manitoba for completing the lab analysis on the crop samples. Jennifer Sokol and Tom Lukowski from CCRS provided very useful comments on the manuscript.

References

BOBER, M.L., WOOD, D., and MCBRIDE, R.A., 1996, Use of digital image analysis and GIS to assess regional soil compaction risk. Photogrammetric Engineering and Remote Sensing, 62, 1397-1404.

BOUMAN, B.A.M., 1991, Crop parameter estimation from ground-based X-band (3-cm wave) radar backscattering data. Remote Sensing of the Environment, 37, 193-205.

BOUMAN, B.A.M., and VAN KASTEREN, H.W.J., 1990, Ground-based X-Band (3-cm wave) radar backscattering of agricultural crops. I. Sugar beet and potato; Backscattering and crop growth. Remote Sensing of the Environment, 34, 93-105.

BRAKKE, T.W., KANEMASU, E.T., STEINER, J.L., ULABY, F.T., and WILSON, E., 1981, Microwave radar response to canopy moisture, Leaf-Area Index, and dry weight of wheat, corn and sorghum. Remote Sensing of the Environment, 11, 207-220.

BRISCO, B., and BROWN, R.J., 1995, Multidate SAR/TM synergism for crop classification in western Canada. Photogrammetric Engineering and Remote Sensing, 61, 1009-1014.

BROWN, R.J., MANORE, M.J., and POIRIER, S., 1992, Correlations between X-, C- and L-band imagery within an agricultural environment. International Journal of Remote Sensing, 13, 1645-1661.

BUSH, T.F., and ULABY, F.T., 1978, An evaluation of radar as a crop classifier. Remote Sensing of the Environment, 7, 15-36.

CLOUTIS, E.A., CONNERY, D.R., MAJOR, D.J., and DOVER, F. J., 1996, Agricultural crop condition monitoring using airborne C-band synthetic aperture radar in southern Alberta, International Journal of Remote Sensing, 13, 2565-2577.

DUSEK, D.A., JACKSON, R.D., and MUSICK, J.T., 1985, Winter wheat vegetation indices calculated from combinations of seven spectral bands. Remote Sensing of the Environment, 18, 255-267.

FERRAZZOLI, P., PALOSCIA, S., PAMPALONI, P., SCHIAVON, G., SOLIMINI, D., and COPPO, P., 1992, Sensitivity of microwave measurements to vegetation biomass and soil moisture content: A case study. IEEE Transactions on Geoscience and Remote Sensing, 30, 750-756.

GARDNER, B.R., BLAD, B.L., THOMPSON, D.R., and HENDERSON, K.E., 1985, Evaluation and interpretation of Thematic Mapper ratios in equations for estimating corn growth parameters. Remote Sensing of the Environment, 18, 225-234.

GAUSMAN, H.W., GERBERMANN, A.H., WIEGAND, C.L., LEAMERR, W., RODRIGUEZ, R.R., and NORIEGA, J.R., 1975, Reflectance differences between crop residues and bare soils. Soil Science Society of America Proceedings, 39, 752-755.

HARDISKY, M.A., DARBER, F.C., ROMAN, C.T., and KLEMA, V., 1984, Remote sensing of biomass and annual net aerial primary productivity of a salt marsh. Remote Sensing of the Environment, 16, 91-106.

HOCHHEIM, K.P., and BARBER, D.G., 1997, The physical properties of wheat and its relationship to canopy backscatter. Geomatics in the Era of Remote Sensing ’97, May 1997 (Ottawa).

HOEKMAN, D.H., 1990, Radar Remote Sensing Data for Applications in Forestry. Doctoral thesis, Wageningen Agricultural University, Wageningen, the Netherlands

HOOGEBOOM, P., 1983, Classification of agricultural crops in radar images. IEEE Transactions on Geoscience and Remote Sensing, 21, 329-336.

JASINSKI, M.F., 1990, Sensitivity of the Normalized Difference Vegetation Index to subpixel canopy cover, soil albedo, and pixel scale. Remote Sensing of the Environment, 32, 169-187.

LILLESAND, T.M., and KIEFER, R.W., 1994, Remote Sensing and Image Interpretation, 3rd edn (New York: John Wiley & Sons).

PRÉVOT, L., CHAMPION, I., and GUYOT, G., 1993, Estimating surface soil moisture and Leaf Area Index of a wheat canopy using a dual-frequency (C and X bands) scatterometer. Remote Sensing of the Environment, 46, 331-339.

ROSENTHAL, W.D., and BLANCHARD, B.J., 1984, Active microwave responses: An aid in improved crop classification. Photogrammetric Engineering and Remote Sensing, 50, 461-468.

SRIVASTAVA, S.K., HAWKINS, R.K., LUKOWSKI, T.I., BANIK, B.T., ADAMOVIC, M., and JEFFERIES, W.C., 1999, RADARSAT image quality and calibration – Update. Advances in Space Research, 23, 1487-1496.

SWAIN, P.H., and DAVIS, S.M. (eds.), 1978, Remote Sensing The Quantitative Approach, (New York: McGraw-Hill).

ULABY, F.T., BATLIVALA, P.P., and BARE, J.E., 1980, Crop identification with L-band radar. Photogrammetric Engineering and Remote Sensing, 46, 101-105.

ULABY, F.T., and BUSH, T.F., 1976, Monitoring wheat growth with radar. Photogrammetric Engineering and Remote Sensing, 42, 557-568.

VAN DER SANDEN, J.J., and HOEKMAN, D.H., 1999, Potential of airborne radar to support the assessment of land cover in a tropical rain forest environment. Remote Sensing of the Environment, 68, 29-40.